Available online at www.sciencedirect.com

ScienceDirect

Procedia CIRP 124 (2024) 644–648

www.elsevier.com/locate/procedia

13th CIRP Conference on Photonic Technologies [LANE 2024], 15-19 September 2024, Fürth, Germany

High-speed X-ray imaging of bulge formation during laser percussion drilling with various polarizations in stainless steel

Lukas Schneller[a,b,*], Manuel Henn[a], Christoph Spurk[c], Alexander Olowinsky[d], Felix Beckmann[e], Julian Moosmann[e], Daniel Holder[a], Christian Hagenlocher[a], Thomas Graf[a]

[a]*Institut für Strahlwerkzeuge IFSW, University Stuttgart, Pfaffenwaldring 43, 70569 Stuttgart Germany*
[b]*Graduate School of Excellence advanced Manufacturing Engineering (GSaME) Nobelstr. 12, 70569 Stuttgart Germany*
[c]*Chair for Laser Technology LLT,RWTH Aachen University, Steinbachstr. 15, 52074 Aachen, Germany*
[d]*Fraunhofer-Institute for Laser Technology ILT, Steinbachstr. 15, 52074 Aachen, Germany*
[e]*Institute of Materials Physics, Helmholtz-Zentrum Hereon, Max-Planck-Str. 1, 21502 Geesthacht, Germany*

* Corresponding author. *E-mail address:* lukas.schneller@ifsw.uni-stuttgart.de

Abstract

Achieving high-quality and high-aspect-ratio micro holes with ultrashort pulse laser percussion drilling remains a challenge. Lateral extensions or bulges in dependence on the polarization of the laser beam have so far only been observed by analyzing metallographically prepared cross-sections and the outlets of the holes. For the first time, we present the use of in-situ synchrotron high-speed X-ray imaging to quantitatively capture the time-resolved growth of these bulges in metals. A laser with a pulse duration of 1 ps and a wavelength of 1030 nm was used to investigate the influence of linear and circular polarization as well as the pulse energy on the shape and orientation of the bulges at increasing depths during the drilling process. The bulges were observed to form perpendicular to the polarization at the start of the drilling process. The observations from X-ray images were confirmed by µCT images of the drilled samples.

Keywords: laser drilling; process observation; high-speed X-ray imaging; polarization; bulge formation

1. Introduction

Drilling with ultrashort pulses with linear polarization can lead to effects like bulging and elliptical hole shape. In case of laser percussion drilling, Nolte et al. [1] observed slit-shaped deformations of the bore hole outlets, which were orthogonally oriented to the polarization. In [1,2] similar slits perpendicular to the polarization were observed at the outlet for samples drilled with helical drilling. Depending on the material and laser diameter, the slits start at a depth of approximately 100 µm to 200 µm. At a similar depth so called “bulging” has already been observed for many different parameter sets [3-6]. Bulging refers to the deviation of a hole from a conical shape, becoming first narrowed and then widened. It is assumed that laser-induced plasma acts as a "secondary drilling source" that widens the hole diameter [7,8]. Transported melt and particles in the borehole may narrow the diameter by redepositing on the sidewall [6,9]. Until now metal samples could only be observed in detail after the drilling process through metallographically prepared cross-sections and by examine the in- and outlet of the hole [1,2,10-14]. The use of in-situ synchrotron high-speed X-ray imaging was demonstrated previously the first time for laser percussion drilling [15]. We are now using this method for the first time to quantify the time-resolved growth of these bulges in metals.

10.1016/j.procir.2024.08.192

2. Experimental Setup

For the experiments described below, an ultrafast laser with a pulse duration of 1 ps, a pulse energy of 150 µJ, a repetition rate of 50 kHz and a beam diameter of 50 µm was used to drill holes in stainless steel. The total drilling time was $t = 10$ s, i.e. a total of $N = 500{,}000$ Pulses. The polarization was adjustable between:

- circular polarization,
- linear polarization perpendicular to the image plane and
- linear polarization parallel to the image plane.

In the following, only the first $t = 2000$ ms of the drilling process and the upper part of the hole are considered, in which bulging occurs for the first time. Each experiment was carried out $n = 3$ times with the same parameters. A synchrotron high-speed X-ray imaging setup, further described in [16] and including a X-ray beam, a scintillator and a high-speed camera was used to capture the drilling progress with a frame rate of 1 kHz, as presented in Fig. 1. The grayscale images obtained are brighter when less material is absorbing the X-rays due to the larger borehole in the Y-direction.

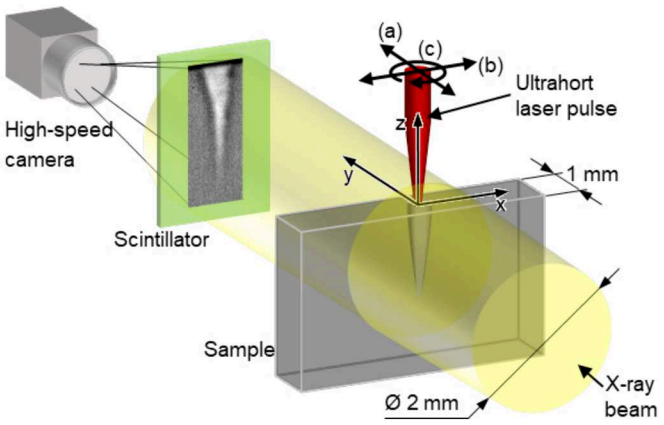

Fig. 1: Setup for X-ray imaging during percussion drilling with ultrashort laser pulses with linear polarization (a) perpendicular to the image plane and (b) parallel to the image plane. (c) Circular polarization.

3. Results

Fig. 2 shows the depth progress up to $N = 102{,}500$ pulses ($t = 2{,}050$ ms) of the upper part of the drilling process for a linear polarization perpendicular to the image plane. In the displayed area at around $N = 7{,}500$ and $N = 17{,}500$ pulses the direction of growth at the bottom of the hole changes and deviates to the right compared to the final hole shape. A detailed discussion of this phenomenon is covered in a future work by Schneller et al. [17]. Bulging appears to start after around $N = 12{,}500$ pulses at a z-position of around $z_b = -250$ µm (Fig. 1 a.) and moves down at a z-position of $z_b = -300$ µm. The constriction above the bulge appears at a z-position of $z_c = -100$ µm (b) and moves down to a z-position of $z_c = -150$ µm after $N = 32{,}500$ pulses.

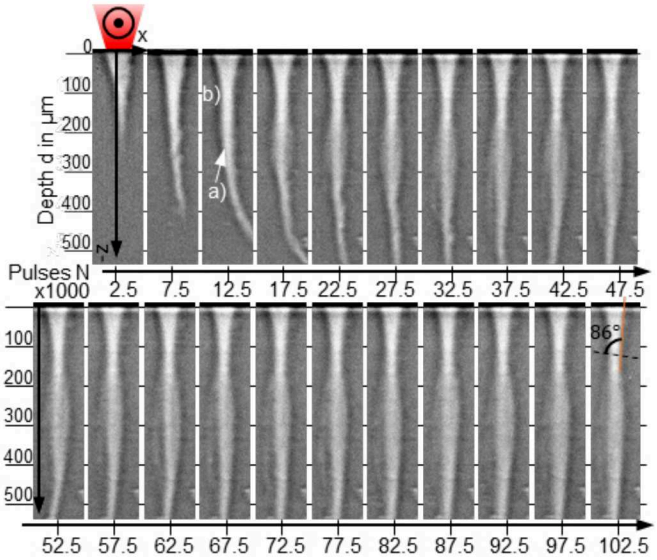

Fig. 2: Bulge formation with polarization perpendicular to the image plane. a) Bulge b) Constriction above the bulge.

Fig. 3 shows the drilling process during the first $N = 102{,}500$ pulses of the upper part of the drilling process with a linear polarization parallel to the image plane. The hole was drilled using the same parameters as shown in Fig. 2, except for the polarization, which resulted in the hole being rotated by 90° around the Z-axis. The bright area in the center of the hole, highlighted with the letter a) in Fig. 3, is caused by the bulging effect visible in Fig. 2. In this plane bulging starts in a later stage of the drilling process and appears to be less pronounced than in the perpendicular plane as shown above in Fig. 1. Both, the constriction and the bulge appear around 50 µm deeper compared to the polarization perpendicular to the image plane shown in Fig. 2.

Fig. 4 shows the bulge formation of a hole drilled with circular polarization. Bulging begins after approximately the same number of pulses as in case of polarization perpendicular to the image plane. The bulge appears to be slightly wider compared to polarization parallel to the image plane, but without the bright area in the middle.

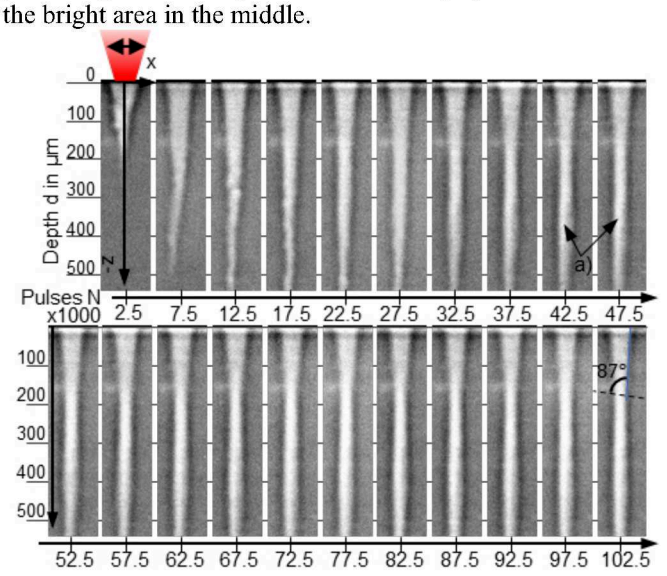

Fig. 3 Bulge formation with polarization parallel to the image plane. a) Bulge in y-direction causes bright area.

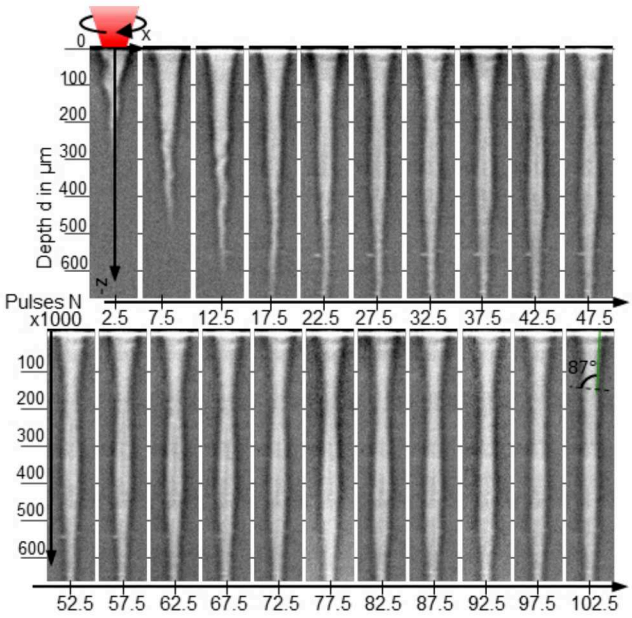

Fig. 4: Bulge formation with circular polarization.

Fig. 5 shows the local maximum width $w_b(t)$ of the bulges and the local minimum width $w_c(t)$ of the constrictions for $n = 3$ experiments for each investigated polarization as a function of applied pulses N. The bulge in direction of the polarization (Fig. 5 blue) appears about 20,000 pulses after the bulge perpendicular to the polarization (Fig. 5 orange). The widths of the bulges for circular polarization (green) and polarization parallel to the image plane (blue) show no significant difference.

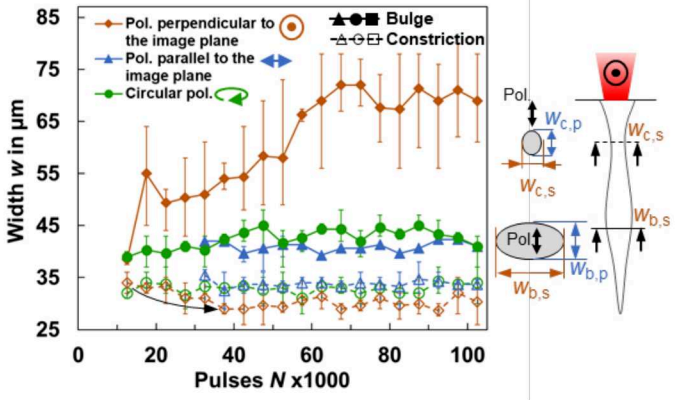

Fig. 5: Maximum width w_b of the Bulge (solid lines) and the minimum width w_c of the constriction (dashed lines) for three different polarizations. Error bars are min/max values. The black arrow indicates a decrease of the constriction width. Right: Non-circular lateral geometry at the bulge and the constriction.

The orange curves in Fig. 5 show that the lateral bore hole geometry is more pronounced in the direction perpendicular to the polarization. Here the bulge is wider compared to the other polarizations, which are displayed as green and blue curves in Fig. 5. From the first appearance of the constriction at N=12,500 pulses until N=37,500 pulses, the constriction in the direction perpendicular to polarization (Fig. 5 black arrow and orange dashed line) decreases from $w_{c,s}$=34 µm to less than 30 µm. This indicates that new material has probably been redeposited on the wall as already presented in the literature [7,18]. For N>40,000 pulses the dimension of the constriction $w_{c,s}$ is narrower than $w_{c,p}$ in the direction parallel to the polarization (Fig. 5 blue dashed line). This will result in a non-circular lateral section at the z-position z_c of the constriction with larger lateral extension in the direction of polarization (Fig. 5 right). At the z-position z_b of the bulge (Fig. 5 solid line), the lateral extension is larger perpendicular to the direction of polarization (Fig. 5 orange). This means, that somewhere between $z_b < z < z_c$ there is a transition point where the lateral geometry is equal in both directions (perpendicular and parallel to the polarization). For the case of perpendicular polarization (orange), the constriction widths $w_c(t)$ vary significantly less over time than the bulge widths $w_b(t)$. Non-circular lateral geometries in the x-y-plane with the major axis perpendicular to the linear polarization have already been observed [2,10,11,19,20]. For micro holes with a diameter of about 1 µm in thin films the major axis was parallel to the polarization [21,22]. The results evidence, that the bulging phenomena requires a significant borehole depth. Linear polarization amplifies bulging perpendicular to the polarization. This indicates, that these amplified bulges result from the multiple reflections of perpendicular-polarized radiation in deeper areas of the hole [1]. Fig. 6 shows the lateral sections in the x-y-plane of the borehole shown in Fig. 2 for different z-coordinates after N=500,000 pulses e.g. t=10 s of drilling, captured by means of µ-CT images. It confirms, that the lateral shape of the borehole in the x-y-plane changes with the z-position. For z>-190 µm the lateral geometry is elongated in the direction of the polarization.

At z=-190 µm the lateral geometry is approximately circular. For z<-190 µm, small bulges appear perpendicular to the polarization highlighted with black arrows in Fig. 6. Similar geometries at outlets have already been observed in [1,2]. With increasing z-coordinate, the bulge width grows and the lateral geometry becomes increasingly irregular. Below the bulge (Fig. 6 z=-530 µm) the cross section in the x-y-plane gets smaller and the bulge perpendicular to the polarization recedes.

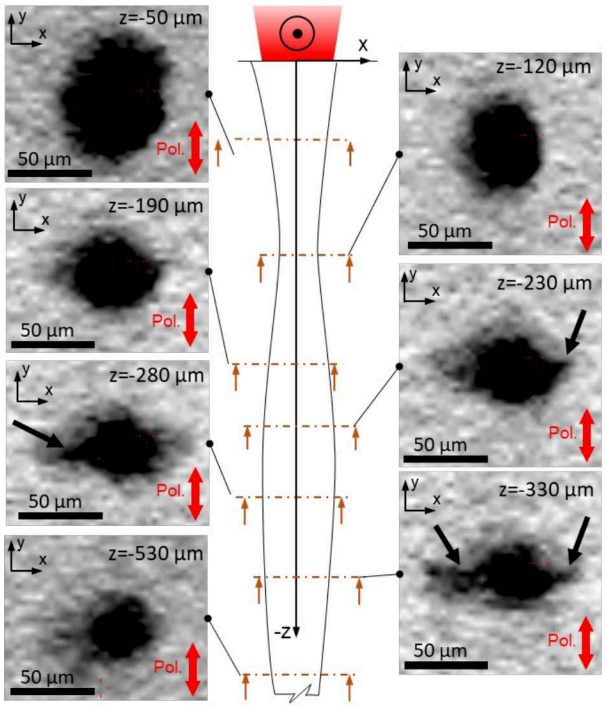

Fig. 6: µ-CTs of the borehole shown in Fig. 2 drilled with linear polarization after N=500,000 pulses. Black arrows highlight the bulges.

4. Discussion

For linear polarization there are two extreme cases inside of a borehole which will be called "S-wall" and "P-wall" as shown in Fig. 7. According to the classic nomenclature in the literature on polarization at inclined incidence [23] the polarization is perpendicular at the S-wall and parallel at the P-wall. Assuming a conical geometry where the angle of incidence increases with depth, especially between a hole depth of 50 µm<d<500 µm, the difference R_S-R_P is high and more than 50 % of the energy is absorbed at the P-wall (Fig. 7 blue) and more than 90 % is reflected at the S-wall (Fig. 7 orange). This leads to the elliptical hole shape in the direction of polarization in the upper part of the hole as already stated above. For further reflections i in the borehole, the angle of incidence decreases as indicated by the orange and blue arrows in Fig. 7. This implies that at the S-wall the absorptivity increases with each reflection, whereas at the P-wall the already significantly lower energy compared to the S-wall is absorbed less with each further reflection.

According to the conical model, the angle of incidence Θ_i would approach 90° at greater depths d. However, it can be seen in Fig. 2 - Fig. 4 above, that at the hole entrance Θ_1 is always about $\Theta_1 \leq 87°$ due to the constriction. This disbalance in the energy distribution between the S-wall and the P-wall leads to the formation of the in Fig. 6 presented geometries. As shown in Fig. 4, bulging is also present when drilling with circular polarization. This can be explained by laser-induced plasma inside of the borehole acting as "a secondary drilling source" [7]. [4]

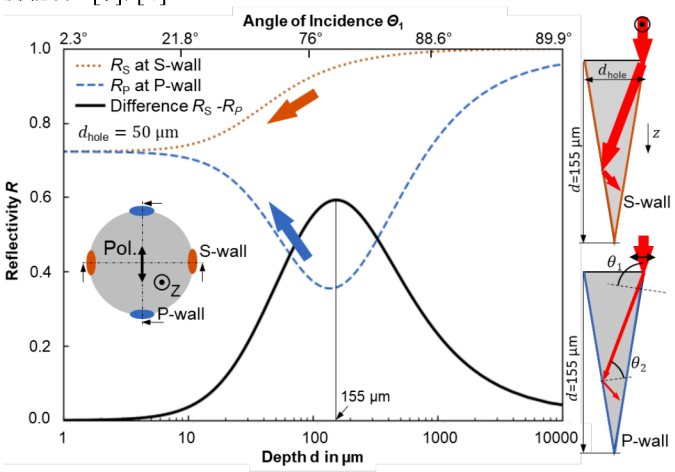

Fig. 7: Reflectivity R over depth d and angle of incidence Θ_1 for S-polarization (orange) and P-polarization (blue). Calculated with d_{hole}=50 µm and n = 2.606, k = 4.956 [24]. For d=155 µm the difference R_S -R_P reaches a maximum.

5. Conclusion

For the first time, high-speed X-ray imaging was used to visualize the time-resolved bulge formation in holes drilled with ultrashort pulse laser percussion drilling with different polarizations in metals. The polarization and angle-dependent reflection leads to an uneven redistribution of energy around the circumference of the borehole. This results in the formation of bulges that appear after a certain stage of the drilling progress, i.e. the initially conical hole changes to a bulge shape after a certain number of pulses. In the upper part of the hole, the presence of a local constriction can be observed. At the constriction, the lateral borehole geometry is elongated in the direction of polarization. In larger hole depth, the lateral elongation rotates by 90°, e.g. perpendicular to linear polarization. This leads to a non-circular cross section of the borehole when drilling with linear polarization. The results shown in this work provide a better understanding of hole formation during deep drilling of metals. This is important for the development of new process strategies to produce high-aspect ratio holes with high quality using percussion drilling.

Acknowledgements

This work was supported by the Landesministerium für Wissenschaft, Forschung und Kunst Baden-Württemberg (Ministry of Science, Research and the Arts of the State of Baden-Württemberg) within the Nachhaltigkeitsförderung (sustainability support) of the projects of the Exzellenzinitiative II. The presented investigations were carried out within the cooperation "Laser Meets Synchrotron" (www.laser-meets-synchrotron.de). The experimental setup and its operation were funded by the Deutsche Forschungsgemeinschaft e.V. (DFG, German Research Foundation) within the framework of the Collaborative Research Centre SFB1120-236616214 "Bauteilpräzision durch Beherrschung von Schmelze und Erstarrung in Produktionsprozessen". The experiments were carried out in cooperation with Helmholtz-Zentrum Hereon in Hamburg at Beamline P07 of DESY PETRA III as part of proposal BAG-20211050 and we would like to thank F. Beckmann, J. Moosmann and all people involved for their support. Thanks to Light Conversion (Vilnius, Lithuania) for providing the ultrashort pulsed laser (Carbide CB3 80).

References

[1] Nolte, S, et al. Polarization effects in ultrashort-pulse laser drilling. (En;en) Appl. Phys. A 1999; 68:5 p. 563–567.

[2] Zhanwen, A, et al. The mechanism of irregular hole-shape formation during ultrafast laser micro-drilling of metals. Appl. Phys. A 2023; 129:2.

[3] Liu, H, et al. Percussion Drilling of Deep Holes Using Picosecond Ultrashort Pulse Laser in Ni-Based Superalloy Coated with Ceramic Thermal Barrier Coatings. (eng) Materials (Basel, Switzerland) 2020; 13:16.

[4] Li, Q, et al. Surface ablation properties and morphology evolution of K24 nickel based superalloy with femtosecond laser percussion drilling. Optics and Lasers in Engineering 2019; 114 p. 22–30.

[5] Luft, A, et al. A study of thermal and mechanical effects on materials induced by pulsed laser drilling. Appl Phys A 1996; 63:2 p. 93–101.

[6] Leitz, K-H, et al. Metal Ablation with Short and Ultrashort Laser Pulses. Physics Procedia 2011; 12 p. 230–238.

[7] Döring, S, et al. Hole Formation Process in Ultrashort Pulse Laser Percussion Drilling. Physics Procedia 2013; 41 p. 431–440.

[8] Klimentov, SM, et al. The role of plasma in ablation of materials by ultrashort laser pulses. Quantum Electron. 2001; 31:5 p. 378–382.

[9] Michalowski, A. Melt Dynamics and Hole Formation during Drilling with Ultrashort Pulses. JLMN 2008; 3:3 p. 211–215.

[10] Foehl, C & Dausinger, F. High precision deep drilling with ultrashort pulses. in *Fourth International Symposium on Laser Precision Microfabrication*: SPIE 2003 p. 346

[11] Wang, R, et al. Polarization effect on hole evolution and periodic microstructures in femtosecond laser drilling of thermal barrier coated superalloys. Applied Surface Science 2021; 537 p. 148001.
[12] Weber, R, et al. Effects of Radial and Tangential Polarization in Laser Material Processing. Physics Procedia 2011; 12 p. 21–30.
[13] Brinkmeier, D, et al. Process limits for percussion drilling of stainless steel with ultrashort laser pulses at high average powers. Appl. Phys. A 2022; 128:1.
[14] Holder, D, et al. Analytical model for the depth progress of percussion drilling with ultrashort laser pulses. Appl. Phys. A 2021; 127:5.
[15] Henn, M, et al. Unveiling laser percussion drilling in metals with ultrashort pulses: insights from high-speed synchrotron x-ray imaging on microhole formation and side channel phenomena. in *Laser-based Micro- and Nanoprocessing XVIII*: SPIE Jan. 2024 - Feb. 2024 p. 19
[16] Lind, J, et al. Influence of the laser cutting front geometry on the striation formation analysed with high-speed synchrotron X-ray imaging. IOP Conf. Ser.: Mater. Sci. Eng. 2021; 1135:1 p. 12009.
[17] Schneller, L, et al. Side channel Formation during Percussion Drilling with Ultrafast Lasers at different Polarizations observed by means of High-speed X-ray Imaging, tbp 2024;
[18] Michalowski, A, et al. Theoretical and experimental studies of ultra-short pulsed laser drilling of steel. in *Laser Sources and Applications II*: SPIE 2014 91350R
[19] Cho, J-H & Na, S-J. Theoretical analysis of keyhole dynamics in polarized laser drilling. J. Phys. D: Appl. Phys. 2007; 40:24 p. 7638–7647.
[20] Zhang, N, et al. Femtosecond laser drilling 100 μm diameter micro holes with aspect ratios > 20 in a Nickel based superalloy. Journal of Materials Research and Technology 2024; 28 p. 1415–1422.
[21] Tao, S, Wu, B& Lei, S. Study of laser beam propagation in microholes and the effect on femtosecond laser micromachining. Journal of Applied Physics 2011; 109:12 p. 123506.
[22] Venkatakrishnan, K, et al. The effect of polarization on ultrashort pulsed laser ablation of thin metal films. Journal of Applied Physics 2002; 92:3 p. 1604–1607.
[23] Hügel, H & Graf, T. Materialbearbeitung mit Laser: Grundlagen und Verfahren. 4th ed. Wiesbaden, Heidelberg: Springer Vieweg; 2022.
[24] Jyothi,J, et al. Optical properties of TiAlC/TiAlCN/TiAlSiCN/TiAlSiCO/TiAlSiO tandem absorber coatings by phase-modulated spectroscopic ellipsometry. Appl Phys A 2017; 123:7.